PCCP

Accepted Manuscript

ROYAL SOCIETY OF CHEMISTRY

www.rsc.org/pccp

Physical Chemistry Chemical Physics
CREATED USING THE RSC LaTeX PCCP ARTICLE TEMPLATE – SEE www.rsc.org/electronicfiles FOR DETAILS
ARTICLE TYPE www. rsc.org/xxxxxx | XXXXXXXX

Unveiling the charge migration mechanism in Na_2O_2: Implications to sodium air batteries.

Rafael B. Araujo[a], **Sudip Chakraborty** *[a], **Rajeev Ahuja**[ab]

Received Xth XXXXXXXXXX 20XX, Accepted Xth XXXXXXXXX 20XX
First published on the web Xth XXXXXXXXXX 200X
DOI: 10.1039/b000000x

Metal air batteries have become a promising candidate for modern energy storage due to their high theoretical energy density in comparison to other storage devices. The lower over potential Na over Li make Na air battery more efficient in terms of battery lifetime. Additionally, the abundance of Na over Li is another advantage plays for Na battery compared to Li battery. Na_2O_2 appears as one of the main products of sodium air battery reactions. The efficiency of air cells is always related with the charge transport mechanisms in the formed product. To unveil these diffusion mechanisms in one of the main products of the cell reaction Na-O_2 we systematically investigate the mobility of charge carriers as well as the electronic structural properties of sodium peroxide. The framework of the density functional theory based on hybrid functional approach is used to study the mobility of charge carries and intrinsic defects in Na_2O_2. Our calculations reveal that the formation of small electron and hole polarons is preferentially occurring over the delocalized state in the crystal structure of the Na_2O_2. The migration of these small polarons displays activation energy of about 0.92 eV and 0.32 eV for the electron and hole polarons respectively. While the analysis of the charged sodium vacancies mobility reveals activation energies of about 0.5 eV. These results suggest that the charge transport in sodium peroxide would mainly occur through the diffusion of hole polarons.

1 Introduction

The monotonic growth of energy storage demand leads to the discovery of batteries with high energy density and low cost production. By capturing atmospheric oxygen, Li-air batteries can become a popular technology as they can store as much energy per volume as gasoline without the need of storing oxidizing agent for the cathode reaction[1,2]. But due to the constrained recharge ability of Li-air batteries motivates the scientific community to replace the anode by sodium (Na) in place of Li without compromising much with the high energy density (Na-air battery: E=2.33 V, wt=1,605 Whg^{-1})[3–5]. The reason behind the limited recharge ability is the instability of the electrolyte in the presence of the reactive superoxide radical that has been produced during the first step of cell discharge. As a consequence of this there is a large overpotential that has been created which is a hindrance behind poor energy efficiency and energy loss as heat[3].In the case of Na-air battery[3], Na forms superoxide (NaO_2) which is much more stable than LiO_2 and the reaction can be reversed while charging due to the restrained decomposition of NaO_2. The charge and discharge process of Na-air battery is kinetically more favourable than the Li-air case because of the fact that the formation and decomposition of NaO_2 is reasonably energy efficient.

Although the limited battery lifetime is a bottleneck for Na air batteries due the negligible energy storage after only the eighth cycle of charge-discharge process leading to the lower capacity[3]. But the lower over potential and abundance of Na over the restricted resources of Li encourage the scientists to overcome the bottleneck of Na air batteries and make them as one of the most promising candidate for the future energy storage applications. The charge transport limitations in Li_2O_2 discharge phase restrict the capacity and the rate constants of Li-air system[6–11], which motivates us to understand profoundly the nucleation, growth, electronic transport and electrocatalysis for the development of the newly found Na-O_2 batteries.

One of the main resulting products of the Na-O_2 cell reaction is sodium peroxide (Na_2O_2)[3] along with sodium superoxide (NaO_2). Both oxides grow on top of a layered cathode material while the battery is discharging and decompose in the charging cycle. The poor conductivity in the discharge product limits the power density of the cell and the surface kinetics are dependent on electronic transport between the surfaces in lithium based systems[6–12]. One important aspect of this investigation is to know whether the same phenomenon happens also in the case of sodium based air batteries.

In this work, we want to envisage the charge transport mechanism in sodium peroxide and to explore the impact of

[a]*Condensed Matter Theory Group, Department of Physics and Astronomy, Box 516, Uppsala University, S-75120 Uppsala, Sweden.*
[b]*Applied Materials Physics, Department of Materials and Engineering, Royal Institute of Technology (KTH), S-100 44 Stockholm, Sweden*
‡Author Correspondance: Fax: +46184713524; Tel: +46728772897; E-mail: sudiphys@gmail.com

charge carriers mobility in Na-O_2 cell performance. We have analysed the electronic structure of non-stoichiometric Na_xO_2. The higher cell potential in these considered systems evolve the sodium defects in the Na_xO_2 structure which leads to the lowering band gap energy. We have also investigated the diffusion mechanism of the charge defects, where the charge transport are mainly governed by the polarons hopping. To obtain accurate electronic and structural properties we have employed the hybrid functional method to describe the exchange and correlation term and many-body perturbation theory (GW) method. The climbing nudge elastic band method (cNEB)[16,17] has been used to determine the energy barrier of defect hopping in all the considered systems.

The predicted band gap value of 4.84eV in Na_2O_2 system using GW method asserts the large insulating behaviour. The excess electron and the hole polaron have been turned into more stable when localised on one peroxide ion. The energy difference between the system with the electron spread in all crystal structure and localised is 1.85 eV, which leads to the fact that thermal vibration will not affect the stability of the polarons. The charge transport investigation that we have undertaken in this work will be quite intuitive for revealing the effect of hopping of polarons (hole and electron) defect.

2 Computational details

The electronic structure calculations of the considered systems throughout this investigation has been performed using projector augmented wave (PAW) implemented Vienna Ab-initio Simulation Package (VASP)[18,19] code within the framework of the density functional theory (DFT). All the calculations have been undertaken using spin polarised formalism and for the exchange correlation functional, Perdew, Burke, and Ernzerhof (PBE)[20] based generalized gradient approximation is used. We have also employed the hybrid functional method in order to overcome the self-interaction error with the the overdelocalized electrons. The hybrid screened functional of Heyd-Scuseria-Ernzerhof (HSE06)[21,22] type which uses a fraction of an exact Hartree-Fock exchange serving to compensate the self-interaction error. The strict convergence tests have been performed which reveal the plane wave cut-off of 600 eV throughout the calculations along with the k-points mesh which has been taken as 6x6x8. Many body perturbation theory by implementing the Hedin's quasi particle approximation has also been used[24–27]. The self-consistent form of the Green's function named scGW is used by considering 320 electronic bands. The idea of performed the scGW calculation is to use the band gap value of Na_2O_2 for adjusting the α mixing parameter from it, which is a frequently used method to set up α[28–30].

The electronic properties of Na_2O_2 have a strong dependence on the value of mixing parameter α of the hybrid functional and hence it has been tested for $\alpha = 0.25, 0.35, 0.48$. The linear variation of the fundamental band gap has been observed with respect to α from 3.99 eV to 4.77 eV and 5.79 eV. While employing scGW0 formalism, the band gap of sodium peroxide has become 4.84 eV. Hence, it has been confirmed that for $\alpha = 0.35$, which consists of 35 % of exact exchange reveal the similar band gap that has been found from scGW methodology. The α value that is taken care of the self-interaction phenomena has been set up according to the recent works[11,28–30].

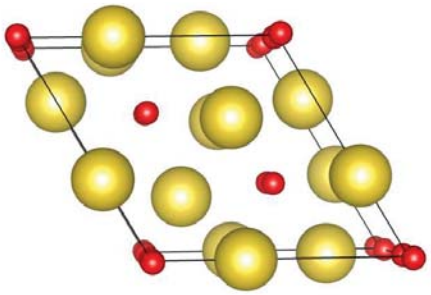

Fig. 1 Crystal structure of sodium peroxide. Yellow balls represent sodium atoms and red balls represent oxygen atoms.

The 2x3x3 supercell consisting of 216 atoms is modelled to investigate the charge transport in sodium peroxide system with a single Γ k-point mesh and this supercell size avoids the interaction between the periodic images. The electron polaron has been formed by adding one more electron in the supercell and the hole polaron has been formed by removing one electron of the supercell. The charge neutrality of the system has been maintained through the compensation of charge background and the optimisation has been performed such a way that the individual atoms are relaxed keeping the supercell shape fixed. The determination of the activation energy is performed using the climbing nudged elastic band (cNEB)[16,17] method by assuming the adiabatic diffusion process of the electron and hole polarons. In addition to this, the diffusion mechanisms of the vacancies are also envisaged using cNEB formalism.

3 Results and Discussions

3.1 Crystal structure

The crystal structure of sodium peroxide is represented in Fig. 1. Na_2O_2 crystallises in a P62m hexagonal space group with the peroxides lying parallel to the C axis, one in each corner of the structure and two more inside[13,14]. Each peroxide is surrounded basically by 9 sodium ions. Tallman[14] has reported a melting point value of 675 °C for Na_2O_2 with a structural transition occurring at 512 °C and another possible transition

around 596 °C. The vibrational modes analysis reveals very low imaginary frequency values what confirms the structural stability. The peroxides O_2^{-2} ions are connected with each other in a anionic molecular sub-lattice bonding with a matrix of Na^+ cations.

Table 2 summarises the lattice parameters and molecular bond distances calculated by using different methods to treat the exchange and correlation terms. A good agreement of the structural parameters emerged from the calculations. However, for the molecular bonding distance of the peroxides in Na_2O_2 the hybrid functional reveals closer values in comparison with the experiment, 1.50 Å for the hybrid calculation and 1.49 Å in the experiment. GGA underestimate the coulomb repulsion and tend to overdelocalize charge densities. With the incorporation of 35 % of the Hartree-Fock exact exchange functional the unphysical self-interaction error is partially cancelled to model correctly the charge density distribution around the oxygen molecules. It leads to a reasonable match of the theoretical boding distance and the experimental value as showed in Tab. 2.

3.2 Electronic structure

In this section we have investigated the electronic properties change when defects are added in the crystal structure of Na_2O_2. Firstly, we have considered a possible discharge mechanism where one electron is inserted in the sodium peroxide creating an electron polaron distortion in the crystal structure. In a second step, we have analysed the electronic structure of sodium peroxide with the inclusion of the hole polaron. Finally, the picture where charged defects V_{Na}^- and common sodium vacancies V_{Na} exist in the lattice of the sodium peroxide has been investigated.

The extra electron shows to be more stable when it is localised in one of the peroxide ion O_2^{-2} forming a O_2^{-3} ion. The energy difference between the systems with the electron spread in the crystal lattice and the one with the localised electron is about 1.85 eV. Furthermore, the bond distance of the formed O_2^{-3} undergoes an expansion from 1.50 Å in the peroxide to 2.30 Å. The anti-bonding character of the new occupied σ^* orbital in the peroxide is the prime reason for the elongation of the bond distance. Other two more observations in the electronic structure calculation are signatures of the electron localisation. The first one is the appearance of a magnetic moment $\mu = 1\ \mu_b$ in the O_2^{-3} ion while it is maintained zero anywhere else in the cell. The second is the very sharp peak close to the valence band maximum showed in Fig. 2 (a) due to the occupation of a LUMO orbital of the O_2, which comes from the deep impurity. The shallow impurities often leads to higher delocalised bands with states crossing the Fermi level. In contrast, deep impurities give rise to sharp and localised states as they are depicted in this work. This results are also observed for Li_2O_2 in the related works[6,12].

Very similar properties are observed with the creation of a hole in this system (lack of one electron). The π^* hole polaron basically localises in one peroxide forming a superoxide, O_2^{-1} and changing the bond distance to 1.30 Å. This bond distance change is a result of the removal of an anti-bonding electron leading to a strengthening of the O_2 bond. It is also observed the emergence of a local magnetic moment due to the rising of an unpaired spin in the O_2^{-1} ion. Analogous results were reported in Li_2O_2 material[11,12,31]. Figure 2 (b) is representing the total DOS of the Na_2O_2 system containing the hole polaron. The small peak at 1.0 eV after the Fermi level characterises a deep acceptor state with a separation of the valence band and spatially localised with the O_2^{-1} exhibits features of a deep centre. Usually, this kind of deep defect leads to a large change of the surround host atoms. Here, the average inter atomic distance between O_2 and the surround sodium atoms is 2.32 Å. For the defect around O_2, this value goes to 2.39 Å confirming the deep character of the hole polaron defect.

Another possibility that has also been analysed here is the formation of V_{Na}^- vacancies and V_{Na} vacancies. In principle conductivity in Na_2O_2 can be quite related to the migration of charged defects where their concentration and mobility appears as dependent parameters. It was observed in Ref.[11] that V_{Li}^- and V_{Li} are the dominant defects in Li_2O_2 (excluding oxygen defects) and with small formation energy in Na_2O_2 contributing to the conductivity. The density of states (DOS) of the supercell with V_{Na}^- vacancy still presents an insulating behaviour with a band gap of 4.71 eV. Basically, most part of the valence and conduction bands in Na_2O_2 are formed by p orbitals coming from the oxygen atoms what explain that the creation of a V_{Na}^- defect did not clearly change the electronic structure of this system. Therefore, even considering a high concentration of V_{Na}^- in the crystal structure of the sodium peroxide it is still going to present as a high band gap material making unlikely the possible band like transport.

The addition of Na defects introduce localised holes in the system that gives rise to the localised states in the band gap (1.76 eV) from the valence band top. The diffusion process of this hole would indeed occurs just when the vacancy migrates from one equilibrium site to another. In fact, we have tried to stabilise the hole polaron far way from the sodium defect. However, the self consistent calculation is always pushing the hole polaron close to the sodium defect.

The possibility of a reasonable change in the electronic structure of Na_2O_2 with V_{Na} defects motivates us to also investigate the configurational properties and how these defects interact between each other. Two Na atoms have been removed from the supercell of Na_2O_2. As a consequence, two peroxide ions oxidised to superoxide state with $\mu = 1\ \mu_b$ of each one. This part of the investigation is carried out with the hybrid functional based exchange correlation functional.

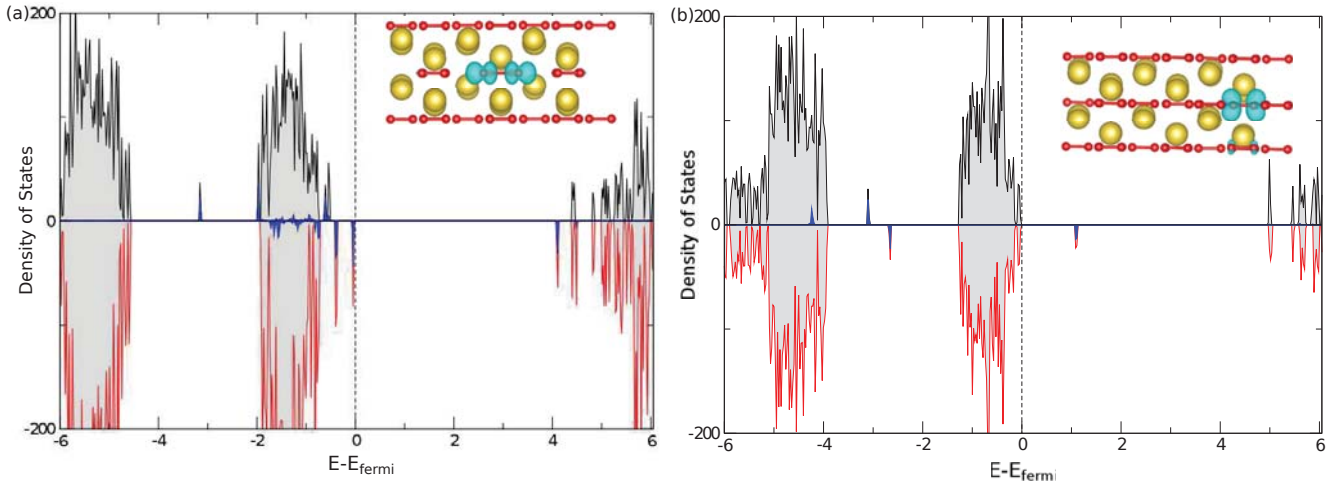

Fig. 2 (a) Total electronic density of states of a supercell with 216 atoms and a hole polaron. Black and brown lines represent the majority and minority spin states. The blue lines are the projected DOS on the local peroxide ion where the hole are located. The dashed lines are the Fermi level. (b) The same as (a) however the the system contains and electron polaron. The picture inside the DOS represents the charge difference of the spin up and down (magnetization density).

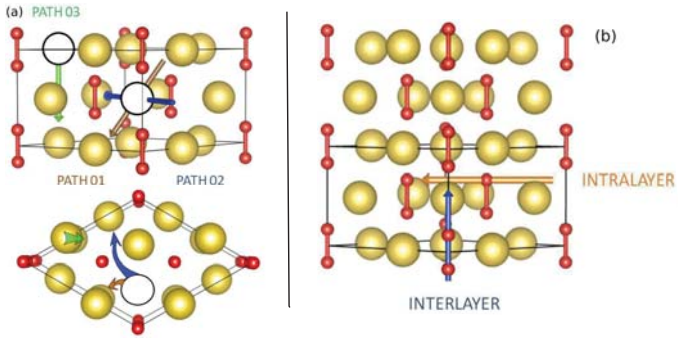

Fig. 3 (a) Schematic representation of pathways 01, 02 and 03 for charged and neutral sodium defects. Here, side and top view are represented, respectively. (b) Schematic representation of the interlayer and intralayer pathways for electron and hole polarons.

Table 1 Computed lattice parameters and band gaps in different approach to the exchange and correlation functional for the sodium peroxide. The GW band gap is also showed here allowing direct comparisons of this quantity. Here, α=0.35.

–	a - b Å	c Å	VOl. Å^3	O-O Å	Band gap (eV)
GGA-GW	6.20	4.7	149.05	1.55	4.84
HSE	6.08	4.40	140.96	1.50	4.77
EXP.	6.22	4.47	149.76	1.49	–

We have placed the defects far away from each other and set up the unpaired spin in the O_2^{-1} ion in two distinct magnetic arrangements, ferromagnetic (FM) and antiferromagnetic (AFM). The revealed energy difference between the AFM and FM magnetic states is small (2 meV), which is not enough to maintain any magnetisation in this structure with temperature effect. The other possibilities are by placing the defects close enough so that there exists an interaction between them. The AFM and FM magnetic states are considered as well. Similar to the first arrangement, the energy difference of the magnetic states is still very small. This arrangement showed to be more stable than the one where the defects have no interaction with an energy difference of 0.4 eV. Therefore, these result suggests that V_{Na} defects tend to form close to each other.

Table 2 Equilibrium defect formation energies (E_f) in eV and concentration (C) in cm^{-3} of the investigated defects. Here, α assume a value 0.35.

	E_f	C
p^+	0.81	2×10^8
p^-	1.82	4×10^{-10}
V_{Na}^-	0.81	3×10^8
V_{Na}	0.74	5×10^9

3.3 Formation energies

Formation energy of several defects has been investigated in this section with the prime goal of deriving the equilibrium concentration C of a defect X in charge state q (X^q). The concentration of a defect X^q in solid state phase can be written as $C(X^q) = Ne^(-E_f/K_bT)$, where E_f is the formation energy and N is the number of sites per unit volume to incorporate the defects[35]. Moreover the formation energy is computed as:

$$E_f(X^q) = E_0(X^q) - E_0(bulk) - \sum_i n_i\mu_i + e\varepsilon_F + E_{MPI} \quad (1)$$

where n_i is the number of atoms of specie i removed or added in the supercell with the defect creation. μ_i is the chemical potential of the cited specie. For sodium it has been set by ion exchange with the anode[11,35]. The Fermi level ε_F is defined as the valence band maximum in the bulk. Moreover, the concentration of charged defects, p^+ and V_{Li}^-, is computed by using the Fermi level that guaranty overall charge neutrality. Table 2 is summarising the equilibrium formation energy and concentration for the investigated defects in this work.

The formation energy of p^+ defects and V_{Na}^- reach a value of 0.81 eV with a charge carrier concentration of the order of 10^8 cm^{-3}. This concentration is about one order of magnitude greater then the reported value in lithium peroxide[11]. However, it is still two orders of magnitude smaller then the intrinsic carrier concentration in silicon (10^{10} cm^{-3} at 300 K). For the neutral vacancy defect (V_{Na}) the revealed formation energy is of the order of 0.74 eV being the most stable defect among the investigated defects here.

3.4 Diffusion Mechanism

Bulk charge transport becomes most important to the kinetics of the cell reaction mainly when particle size in top of the positive electrode increases. To explore charge transport mechanisms in Na_2O_2, the activation energy-barriers are computed using electronic structure theory for the hopping of p^+, p^-, V_{Na}^- and V_{Na}. Then, three different mechanisms are proposed for charge transport: diffusion of charge by V_{Na}^- and V_{Na}, transport through small electron polarons and migration of small hole polarons.

We firstly have investigated the activation barriers of V_{Na}^- and V_{Na} defects hopping from one equilibrium point to another. In this case, three different pathways are considered as depicted in Fig. 3(a) and the cNEB method has been used to determine the activation energy values. Table 4 is summarising these results. Path 03 has revealed very high activation energies for both the sodium defects (V_{Na}^- and V_{Na}). Therefore, migration mechanisms of sodium defects would unlikely take place through this path. The results for the paths 01 and 02 are mainly discussed in the next part of this work.

The activation energy of V_{Na} defects reach 0.52 eV for the most likely pathway as showed in Tab. 4. The energetic difference between the activation energy computed in paths 01 and 02 is 0.12 eV, which is enough to make the diffusion process to be taken place along the path 01. Concerning to the charged defect, the computed activation energies are very similar for paths 01 and 02. This difference suggests that both pathways present close diffusion coefficients. Moreover, path 01 involves an in-plane and out-plane hopping and together with path 02 they would create a collective effect leading to a three dimensional diffusion process for this defect.

Comparing the reported results for the energy barriers hopping of V_{Li}^- in Li_2O_2, which is 0.33 eV[11] with the computed values for the sodium peroxide (0.51 eV), one can observe that the sodium ion migration in Na_2O_2 is going to happen slower than the diffusion of lithium ions in Li_2O_2. The difference in the activation energy is of the order of 0.2 eV. The one possibility is related to the crystal structure difference between Na_2O_2 and Li_2O_2 leading to pathways with distinct diffusion properties. The other possible reason can be the bigger atomic radius of the the sodium ions when compared with Li ions, which leads to a greater electrostatic interaction between the neighbours atoms for the Na case producing higher activation energy barriers.

The variation of the activation barriers with α (hybrid functional mixing parameter) has also been investigated. The change of the exact Hartree-Fock mixing does not have any effect in the activation energy barriers value for the vacancies hopping. In average with the change of α the activation energy undergoes a transformation of about 0.02 eV. In the most critical case, the charged sodium vacancy experiences a transformation of the activation energy from 0.55 eV to 0.50 eV when α goes from 0.25 to 0.35. Basically, for the diffusion of V_{Na}^- and V_{Na} defects, a split of hole polarons in different peroxide sites has not been observed . Even in the case of V_{Na}, which consists of V_{Na}^--p^+ bound pair, our calculations show that in the transition state, the polaron will be localised in one of the peroxide molecules. Therefore, the higher value of α does not change the total energy of the transition state much and it leads to an independent activation energy with respect

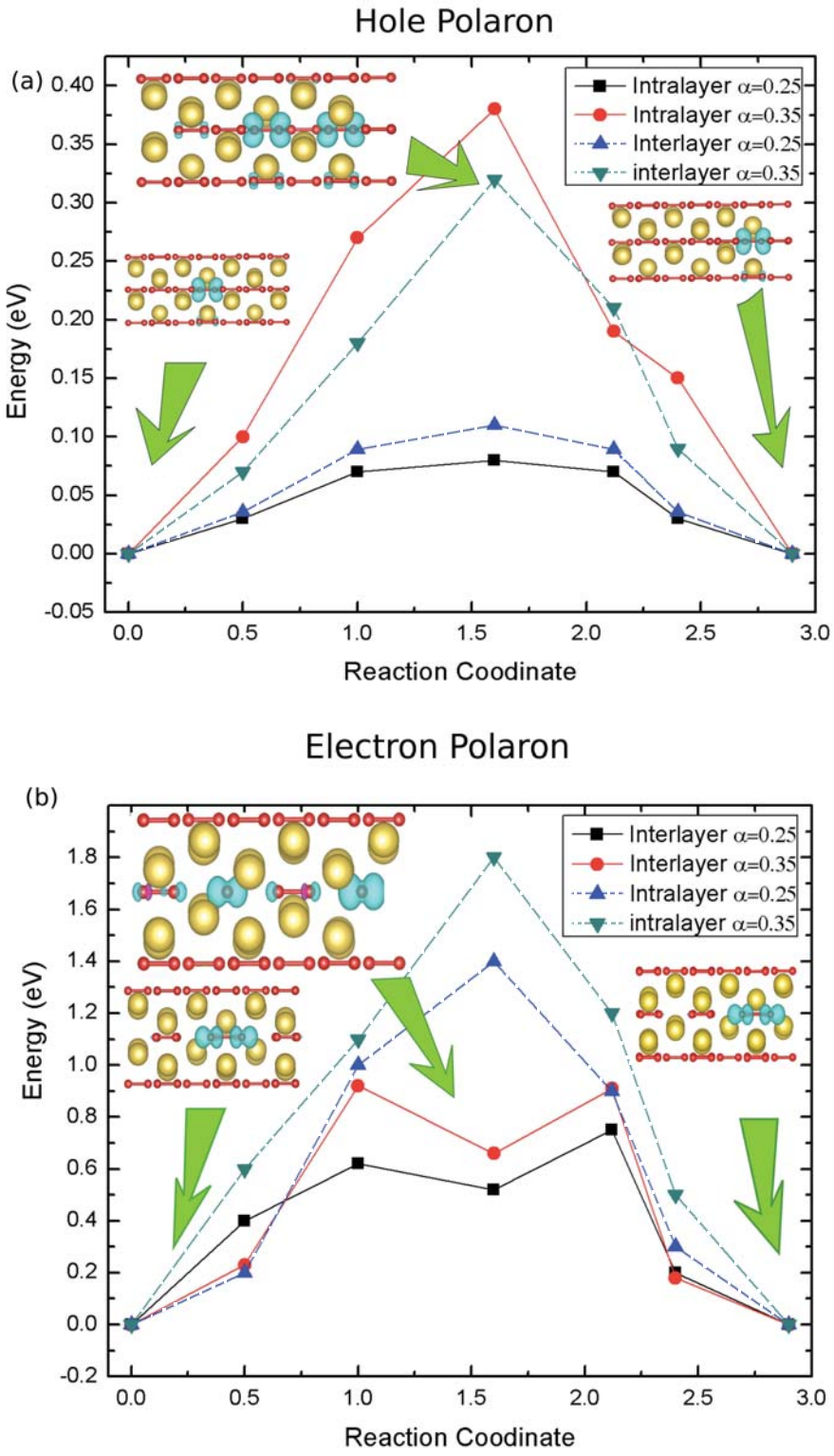

Fig. 4 Activation energy barriers for the hole and electron polaron. Distinct mixing parameters are considered for this calculation. In (a) dashed lines represents Interlayer path and in (b) dashed lines represent the intralayer path. The pictures inside Figs. (a) and (b) are representing the density of magnetisation for the sodium peroxide with one hole (a) and electron (b) polaron in the most likely pathway. These showed density of magnetisation consider 35 % of exact exchange. The red balls are representing oxygen atoms and the yellow balls are representing sodium atoms. There, one can see that both, hole polaron and electron polaron are well localised in one peroxide ion in the equilibrium points. For the transition states it appears delocalised.

Table 3 Summary of the activation energy barriers (E_a) for the vacancy defects V_{Na}^{-} and V_{Na}. This results were calculated by using the hybrid functional with 35 % of exact exchange.

–	–	E_a (eV)	–	E_a (eV)
Path 01	V_{Na}^{-}	0.51	V_{Na}	0.52
Path 02	V_{Na}^{-}	0.50	V_{Na}	0.64
Path 03	V_{Na}^{-}	1.92	V_{Na}	1.99

Table 4 Summary of the activation energy barriers (E_a) of the hole (H. polaron) and electron (E. polaron) polaron. Here, the mixing parameter α assumes 0.25 and 0.35.

		E. polaron (eV)	H. polaron (eV)
Interlayer	25 %	0.75	0.11
	35 %	0.92	0.32
Intralayer	25 %	1.40	0.08
	35 %	1.80	0.38

to the mixing parameter.

The activation energy barriers associated with the holes and electron polarons are also computed. The influence of these quantities to the charge transport in sodium peroxide is analyzed as well. Here, two different pathways as described in Figure 3 (b) have been chosen as the most probable ones, an interlayer and an intralayer similar to lithium peroxide [12,31]. In the sodium peroxide structure the O_2^{-2} ions are aligned parallel to each other in the C direction and opens a possible diffusion channel. The hole and electron polarons with should reveal an smaller activation energy barrier to hope from one peroxide to another, which leads to a distinct behaviour than in the case of Li_2O_2.

Figure 4 (a) is representing the activation energies of the hole polaron migration for the different pathways and mixing parameters. For the intralayer pathway the hole polaron activation energy goes from 0.08 eV to 0.38 eV with α change from 0.25 to 0.35 and for the interlayer it undergoes a transformation from 0.11 eV up to 0.32 eV for the same mixing parameter variation. This behaviour is also observed for lithium peroxide in Ref. [11] when the activation energy for α=0.25 in the intralayer pathway reveals a value around 0.1 eV and 0.71 eV with α=0.48. This dependence with the mixing parameter comes from the splitting of the hole polaron in the transition state. The delocalisation of the hole leads to partial occupied orbital of subsequent peroxides. Increasing the mixing parameter of the hybrid functional also increase the delocalisation of the polaron. The 0.32 eV energy barrier that has been revealed by the interlayer path is lower in energy then the 0.38 eV showed in the intralayer calculation with a discrepancy of about 0.06 eV. However, the activation energy difference is not really great (0.06 eV) allowing migration process occur in both directions. A very close trend of the activation energy in the case of hole polaron migration has been predicted for sodium peroxide and also was reported by Radin *et al.* [11] in the intralayer path. It is an expected behaviour due to the similarity regarding this pathway as far both the materials Li_2O_2 and Na_2O_2 are concerned.

The observed discrepancy of the activation energy in the interlayer path between the lithium and sodium peroxide is quite evident. This difference is a consequence of structural properties that results in a very different surroundings for Na and Li ions in their reciprocal hosts for the interlayer path. The fact that O_2^{-2} is lined up in the sodium peroxide crystal structure decrease the interlayer activation energy of the hole polaron in comparison with Li_2O_2. Therefore, the hole polaron migration in Na_2O_2 reveals different characteristics in compare with the lithium chemistry.

Our calculations for the electron polaron determine the activation energies of the order of 0.92 and 1.80 eV for the inter and intralayer pathways. The difference between the energy barriers computed in both the pathways is 0.9 eV more than the hole polaron case that leads to an anisotropic migration process for the excess electron in sodium peroxide. Comparing the activation energies with distinct α values (0.25 and 0.35) the calculated barriers undergo a change of about 0.17 eV and 0.4 eV for the the inter and intralayer pathways respectively. Figure 4 (b) shows the result for the intralayer and interlayer activation energies of the extra electron hopping.

The shape difference presented in Fig. 4 (b) of the activation barrier in the inter and intralayer pathways is a result of the crystal structure of the sodium peroxide and the p_z character of the extra electron. In the interlayer path of O_2^{-2} ions is allowing a stronger electronic coupling of the peroxide where the extra electron is located and its next neighbour. The addition of one more electron forming O_2^{-3} ion leads to a stretching of its bond distance. One of the oxygen atoms (O_2^{-3}) appears quite close to the next peroxide forming a local minimum for the excess electron.

The diffusion mechanisms of the excess electron polaron in the Na_2O_2 crystal structure have showed quite different properties from the reported ones in Li_2O_2 by Kang *et al.* [31] and Garcia-Lastra *et al.* [12]. With the standard hybrid functional [31], the activation barriers are computed as 0.54 and 0.66 eV for the inter and intralayer pathways. On other hand, Ref. [12] predicts the activation energies of 1.40 and 1.47 eV for the same paths but using DFT+U method. The main difference showed by the electron hopping in the interlayer path for the Na_2O_2 and Li_2O_2 is an result of a stronger electronic interaction of the peroxide ions due to structural symmetry features revealed by the sodium peroxide.

An activation barrier of 0.5 eV has been found for the diffusion of charged defects (V_{Na}^{-}) in sodium peroxide for the

most probable pathway. This activation barrier leads to a conductivity of the order of 10^{-22} S/cm at room temperature, where the conductivity has been computed by the equation $\sigma = \frac{Ce^2a^2\nu}{k_BT} exp(-E_a/k_BT)$[38]. Here, a is the distance between the hopping sites, ν is the related vibrational frequencies (10^{-13} Hz), E_a is the activation energy, T is the temperatures, k_B is the Boltzmann constant and C is the concentration. For a brief comparison, the intrinsic ionic conductivity in Li_2O_2 reported by Radin et. al.[11] is predicted to be of the order of 9×10^{-19} S/cm where the target value for optimal performance of the battery is 10^{-11} S/cm. The predicted ionic conductivity for sodium peroxide is still smaller compared to the reported in Ref.[11]. The electron hole activation energies have been predicted as 0.92 eV due to the coupling of the lined up peroxide atoms in the crystal structure of Na_2O_2. The activation barrier of the electron polaron is smaller than the reported values for Li_2O_2 (1.4 eV)[12] leading to a very small conductivity at room temperature 10^{-46} S/cm. These results indicate that the electron polaron will not play any significant role in the charge transport of sodium peroxide.

The charge carriers that primary responsible for the charge diffusion in Na_2O_2 is the hole polaron. The activation energies of the hole polaron reach values as great as 0.32 eV and 0.38 eV for the inter and intralayer paths characterising an anisotropic diffusion transport. Moreover, it leads to an intrinsic conductivity value of the order of 10^{-19} S/cm, which is much greater than the sodium vacancy and electron polaron.

4 Conclusions

In order to explore the diffusion mechanisms and the mobility of charge carriers in one of the main products of the cell reaction Na-O_2 in Na air battery, we have done a systematic density functional theory based electron structure investigation. The formation of small polarons has been found in Na_2O_2 along with the fundamental band gap of 4.84 eV by using GW approach. Pathway 01 as the most possible one for the sodium defects diffusion and the diffusion of charged sodium defects does reach 0.50 eV barrier. The electron polaron is hopping through the interlayer paths and presenting an activation energy of 0.92 eV. The hole polaron is showing an almost isotropic diffusion with barrier activation of 0.32 eV and 0.38 eV for the interlayer and intralayer paths respectively. These results suggest that the main responsible to the charge diffusion process in sodium peroxide is attributed to the hole polaron migration. This mechanistic study of charge migration pathway would initiate a lot more effort from the experimental counterpart in near future in order to develop new way to increase the life time of Na air batteries.

5 Acknowledgement

R.B.A is thankful to Erasmus Mundus for the doctoral fellowship. We would like to acknowledge the Carl Tryggers Stiftelse for Vetenskaplig Forskning (CTS), Swedish Research Council (VR), Swedish Energy Agency for financial support. SNIC, HPC2N and UPPMAX are acknowledged for providing computing time.

References

1 P. G. Bruce, S. A. Freunberger, L. J. Hardwick and J. M. Tarascon, Nat. Mater., 2012, **11**, 1929.
2 B. D. McCloskey, J. M. Garcia and A. C. Luntz, J. Phys. Chem. Lett., 2014, **5** (7), 12301235.
3 P. Hartmann, C. Bender, M. Vračar, A. K. Drür, A. Garsuch, J. Janek and P. A. Adelhelm, Nat. Mater., 2013, **12**, 228 232.
4 P. Hartmann, D. Gürbl, H. Sommer, J. Janek, W. C. Bessler and P. Adelhelm, J. Phys. Chem. C, 2014, **118**, 1461.
5 P. Hartmann, C. L. Bender, J. Sann, A. K. Drür, M. Jansen, J. Janek and P. A. Adelhelm, Phys. Chem. Chem. Phys. 2013, **15**, 11661.
6 J. Kang, Y. S. Jung, S. Wei and A. C. Dillon, Phys. Rev. B, 2012, **85**, 035210.
7 V. Viswanathan, K. S. Thygesen, J. S. Hummelshøj, J. K. Nørskov, G. Girishkumar, B. D. McCloskey and a. C. Luntz, J. Chem. Phys., 2011, **135**, 214704.
8 P. Albertus, G. Girishkumar, B. McCloskey, R. S. Sanchez- Carrera, B. Kozinsky, J. Christensen and A. C. Luntz, J. Electrochem. Soc., 2011, **158**, A343.
9 S. K. Das, S. Xu, A. H. Emwas, Y. Y. Lu, S. Srivastava and L. A. Archer, Energy Environ. Sci., 2012, **5**, 8927.
10 Y. C. Lu and Y. Shao-Horn, J. Phys. Chem. Lett., 2013, **4**, 93 99.
11 M. D. Radina and D. J. Siegel, Energy Environ. Sci., 2013, **6**, 2370.
12 J. M. Garcia-Lastra, J. S. G. Myrdal, R. Christensen, K. S. Thygesen and T. Vegge, J. Phys. Chem, 2013, **117**, 5568-5577.
13 H. A. Wriedt, Bull. Alloy Phase Diagrams 1987, **8** (3), 234246.
14 R. L. Tallman and J. L. Margrave , J. lnorg. Nucl. Chem., 1961, **21**, 40.
15 S. Kang, Y. Mo, S. P. Ong, and G. Ceder, Nano Lett., 2014, **14**, 10161020.
16 H. Jonsson, G. Mills, and K. W. Jacobsen, in Classical and Quantum Dynamics in Condensed Phased Simulations, edited by B. J. Berne, G. Ciccotti, and D. F. Coker (World Scientific, River Edge, NJ, 1998), p. 385.

17 G. Henkelman and H. J. Jonsson, Chem. Phys. 2000, **113**, 9978.

18 G. Kresse, J. Hafner, Phys. Rev. B, 1993, **47**, 558.

19 G. Kresse, J. Hafner, Phys. Rev. B, 1996, **54**, 11169.

20 J. P. Perdew, K. Burke, M. Ernzerhof, Phys. Rev. Lett., 1996, **77**, 3865.

21 Heyd, G. E. Scuseria, and M. Ernzerhof, J. Chem. Phys., 2003, **118**, 8207.

22 Heyd, G. E. Scuseria, and M. Ernzerhof, J. Chem. Phys., 2006, **124**, 219906.

23 S. L. Dudarev, G. A. Botton, S. Y. Savrasov, C. J. Humphreys, A. P. Sutton, Phys. Rev. B, 1998, **57**, 1505.

24 M. S. Hybertsen and S. G. Louie, Phys. Rev. B, 1985, **32**, 7005.

25 M. S. Hybertsen and S. G. Louie, Phys. Rev. B, 1986, **34**, 5390.

26 M. Shishkin and G. Kresse, Phys. Rev. B, 2007, **75**, 235102.

27 M. Shishkin and G. Kresse, Phys. Rev. B, **2006**, 74, 035101.

28 W. R. L. Lambrecht, Phys. Status Solidi B, 2011, **248**, 1547 1558.

29 A. Alkauskas, P. Broqvist and A. Pasquarello, Phys. Status Solidi B, 2011, **248**, 775789.

30 M. Choi, A. Janotti and C. G. Van de Walle, J. Appl. Phys., 2013, **113**, 044501.

31 S. P. Ong, Y. Mo and G. Ceder, Phys. Rev. B: Condens. Matter Mater. Phys., 2012, 85, 081105.

32 M. Nolan, G. M. Watson, Surf. Sci., 2005, **586**, 2537.

33 M. Nolan, G. W. Watson, J. Chem. Phys., 2006, **125**, 144701.

34 V. Pardo, W. E. Pickett, Phys. Rev. B, 2008, **78**, 134427.

35 C. G. Van de Walle and J. Neugebauer, J. Appl. Phys., 2004, **95**, 3851.

36 A. Droghetti, C. D. Pemmaraju, S. Sanvito, Phys. Rev. B 2010, **81**, 092403.

37 Y. I. Jang, B. J. Neudecker, and N. J. Dudney, Electrochem. Solid-State Lett., 2001, **4**, A74.

38 R. J. D. Tilley, Defects in Solids, John Wiley Sons, Inc., 2008.